

PAPER • OPEN ACCESS

Input–output description of microwave radiation in the dynamical Coulomb blockade

To cite this article: J Leppäkangas *et al* 2014 *New J. Phys.* **16** 015015

View the [article online](#) for updates and enhancements.

Related content

- [Readout methods and devices for Josephson-junction-based solid-state qubits](#)
G Johansson, L Tornberg, V S Shumeiko *et al.*
- [Majorana fermions coupled to electromagnetic radiation](#)
Christoph Ohm and Fabian Hassler
- [Cavity QED with hybrid nanocircuits: from atomic-like physics to condensed matter phenomena](#)
Audrey Cottet, Matthieu C Dartailh, Matthieu M Desjardins *et al.*

Recent citations

- [Microwave photonics with superconducting quantum circuits](#)
Xiu Gu *et al*
- [Emission of Nonclassical Radiation by Inelastic Cooper Pair Tunneling](#)
M. Westig *et al*
- [Creating photon-number squeezed strong microwave fields by a Cooper-pair injection laser](#)
Martin Koppenhöfer *et al*

Input–output description of microwave radiation in the dynamical Coulomb blockade

J Leppäkangas^{1,3}, G Johansson¹, M Marthaler² and M Fogelström¹

¹ Microtechnology and Nanoscience, MC2, Chalmers University of Technology, SE-412 96 Göteborg, Sweden

² Institut für Theoretische Festkörperphysik and DFG-Center for Functional Nanostructures (CFN), Karlsruhe Institute of Technology, D-76128 Karlsruhe, Germany
E-mail: juha.leppakangas@chalmers.se

Received 14 September 2013, revised 4 November 2013

Accepted for publication 3 December 2013

Published 10 January 2014

New Journal of Physics **16** (2014) 015015

[doi:10.1088/1367-2630/16/1/015015](https://doi.org/10.1088/1367-2630/16/1/015015)

Abstract

We study microwave radiation emitted by a small voltage-biased Josephson junction connected to a superconducting transmission line. An input–output formalism for the radiation field is established, using a perturbation expansion in the junction's critical current. Using output field operators solved up to the second order, we estimate the spectral density and the second-order coherence of the emitted field. For typical transmission line impedances and at frequencies below the main emission peak at the Josephson frequency, radiation occurs predominantly due to two-photon emission. This emission is characterized by a high degree of photon bunching if detected symmetrically around half of the Josephson frequency. Strong phase fluctuations in the transmission line make related nonclassical phase-dependent amplitude correlations short lived, and there is no steady-state two-mode squeezing. However, the radiation is shown to violate the classical Cauchy–Schwarz inequality of intensity cross-correlations, demonstrating the nonclassicality of the photon pair production in this region.

³ Author to whom any correspondence should be addressed.



Content from this work may be used under the terms of the [Creative Commons Attribution 3.0 licence](https://creativecommons.org/licenses/by/3.0/).

Any further distribution of this work must maintain attribution to the author(s) and the title of the work, journal citation and DOI.

1. Introduction

In a resistive environment, charge tunneling across a voltage-biased Josephson junction (JJ) triggers simultaneous microwave emission [1, 2], that carries away all or some of the gained electrostatic energy. For voltages below the superconducting gap, $eV < \Delta$, the radiation is purely due to Cooper-pair tunneling since charge tunneling via excitation of quasiparticles is energetically forbidden. This mechanism leads to spectroscopically sharp features, which can be used for the probing of environmental energy levels [3–5], as photon absorption by the environmental modes influences the simultaneously measurable dc-current. A novel idea is to use the voltage-biased small JJ as a source of nonclassical microwave radiation, i.e. to convert the applied dc-voltage into correlated microwave photons [6, 7]. This has recently stimulated theoretical studies of the emitted microwave field [7–10].

In this paper, we investigate microwave radiation produced in a dc-voltage-biased superconducting transmission line that is terminated by a small JJ. We establish an input–output formalism for the field operators in the transmission line. In this formalism, the electric current across the JJ acts as a nonlinear and time-dependent boundary condition for the microwave field [11, 12]. We solve this perturbatively as a power series in the junction’s critical current [7], and give explicit expressions for the output field operators up to the second order in the critical current. Assuming thermal equilibrium of the input field we recover the limit of incoherent Cooper-pair tunneling [1, 2], where microwave emission is due to an incoherent sequence of Cooper-pair tunneling events. The photon flux has been studied recently experimentally in this regime, [6] and it was shown that the radiation at voltages below the Josephson frequency, for typical transmission-line impedances, is due to simultaneous two-photon emission. Using the formalism established in this paper, we also study the nonclassicality of the photon pair production occurring in this region.

Using field operators up to the second order in the junction’s critical current, we derive analytical expressions for the first- and second-order (photon) coherences for typical transmission lines. We reproduce results for the photon-flux density and simultaneous electric current, previously derived using the $P(E)$ -theory [2, 6]. Further, the emission characteristic below the Josephson frequency is shown to be highly bunched if detected symmetrically around half the Josephson frequency, eV/h . We then further study the nonclassicality of the photon pair production occurring below the Josephson frequency [7]. Strong phase fluctuations in the transmission line make phase-dependent nonclassical amplitude correlations short lived, and lead to a vanishing two-mode squeezing, in the steady state. We thus proceed to prove the nonclassicality of the radiation in a different way, considering the classical Cauchy–Schwarz inequality of intensity cross-correlations, a nonclassicality test that is not affected by dephasing. Using the developed methods, we derive an equivalent inequality but expressed in terms of $P(E)$ -functions. This is used to show that the emitted photons below the Josephson frequency violate the inequality, demonstrating the nonclassicality of the photon pair production in this region.

The paper has the following structure. In section 2 we introduce the model we use to describe the radiation in the transmission line, and the nonlinear and time-dependent boundary condition created by the JJ. In section 3, we derive the solution by establishing a perturbation expansion in the junction’s critical current. In section 4, we derive results for the microwave spectral density in the used leading-order approximation, whose validity is also addressed in this section. Higher-order coherences and the nonclassicality of the output radiation are investigated in section 5. The technical details of the calculations are given in appendices A–D.

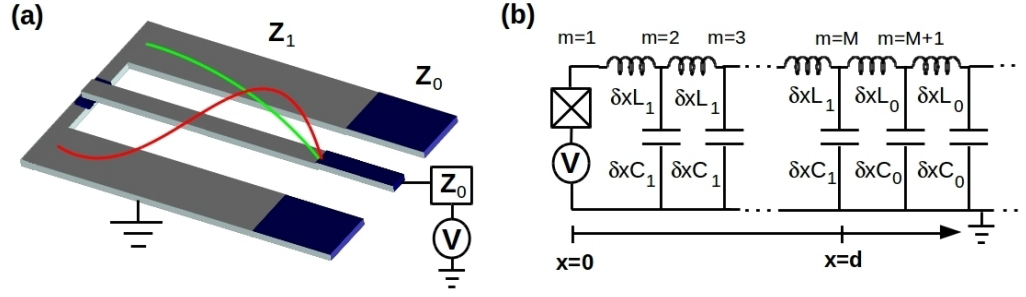


Figure 1. (a) We consider a dc-voltage-biased transmission line terminated by a small JJ. We allow for a step-like change in the characteristic impedance from Z_0 to Z_1 , supporting the depicted modes of a $\lambda/4$ resonator. (b) The equivalent circuit model consists of an infinite series of capacitors $\delta x C_i$ and inductors $\delta x L_i$, where δx is a small discretization width, that is allowed to approach zero ($\delta x M = d$), in parallel with a JJ (crossed box). We have $Z_i = \sqrt{L_i/C_i}$. The upper conductor consists of series of islands, each assigned a counting parameter m .

2. The system and the model

Our system consists of a dc-voltage-biased transmission line terminated by a small JJ, figure 1(a). We consider explicitly two types of environments: (i) a semi-infinite transmission line (i.e. $Z_0 = Z_1$); and (ii) a semi-infinite transmission line with a $\lambda/4$ cavity (i.e. $Z_1 > Z_0$). Case (i) allows for analytical solutions, while case (ii) enhances the output radiation at the cavity resonances, which is important in experiments.

2.1. Heisenberg equations of motion and quantization of the electromagnetic (EM) field

Following [12], we model the system using a discretized circuit model, depicted in figure 1(b). The total Lagrangian of the system can be decomposed as

$$\mathcal{L} = \mathcal{L}_c + \mathcal{L}_f + \mathcal{L}_J. \quad (1)$$

The cavity ($0 < x < d$) and the free space ($x > d$) Lagrangians are, respectively [11]

$$\mathcal{L}_c = \sum_{m \geq 1}^M \frac{\delta x C_1 \dot{\Phi}_m^2}{2} - \sum_{m \geq 2}^N \frac{(\Phi_m - \Phi_{m-1})^2}{2L_1 \delta x}, \quad (2)$$

$$\mathcal{L}_f = \sum_{m > M} \frac{\Delta x C_0 \dot{\Phi}_m^2}{2} - \sum_{m \geq M} \frac{(\Phi_m - \Phi_{m+1})^2}{2L_0 \Delta x}. \quad (3)$$

Here $\Phi_m(t)$ is the magnetic flux of node m , see figure 1(b). The JJ is described by the term

$$\mathcal{L}_J = \frac{C_J \dot{\Phi}_1^2}{2} + E_J \cos \left(2\pi \frac{\Phi_1 - \Phi_V}{\Phi_0} \right). \quad (4)$$

Here C_J is the junction's capacitance, E_J is the Josephson coupling energy, $\Phi_0 = h/2e$ is the flux quantum and the dc-voltage bias results in the term $\Phi_V = Vt$.

We consider the Heisenberg equations of motion in the continuum limit $\delta x \rightarrow 0$. Inside each region, free space ($i = 0$) or cavity ($i = 1$), one obtains a Klein–Gordon equation

$$\ddot{\Phi}(x, t) = \frac{1}{L_i C_i} \frac{\partial^2 \Phi(x, t)}{\partial x^2}. \quad (5)$$

Here $\Phi(x, t)$ is the position-dependent magnetic flux. We write down a solution for the cavity region as ($0 < x < d$)

$$\Phi(x, t) = \sqrt{\frac{\hbar Z_1}{4\pi}} \int_0^\infty \frac{d\omega}{\sqrt{\omega}} \left[a_{\text{in}}^c(\omega) e^{-i(k_\omega^c x + \omega t)} + a_{\text{out}}^c(\omega) e^{-i(-k_\omega^c x + \omega t)} + \text{h.c.} \right]. \quad (6)$$

Here $Z_1 = \sqrt{L_1/C_1}$ is the corresponding characteristic impedance and $k_\omega^c = \omega \sqrt{C_1 L_1}$ the wave number. Similarly, we write the free-space solution as ($x > d$)

$$\Phi(x, t) = \sqrt{\frac{\hbar Z_0}{4\pi}} \int_0^\infty \frac{d\omega}{\sqrt{\omega}} \left[a_{\text{in}}^f(\omega) e^{-i(k_\omega^f x + \omega t)} + a_{\text{out}}^f(\omega) e^{-i(-k_\omega^f x + \omega t)} + \text{h.c.} \right]. \quad (7)$$

The in-field creation operators of photons, $a^\dagger(\omega)$, and the annihilation operators, $a(\omega)$, satisfy the commutation relation [13]

$$\left[a_{\text{in}}(\omega), a_{\text{in}}^\dagger(\omega') \right] = \delta(\omega - \omega'). \quad (8)$$

As a consistency check of our theory, we will show that (8) is satisfied also for the out field operators.

2.2. Boundary conditions for the EM field

The boundary conditions appear at the JJ ($x = 0$) and at the possible discrete change of the transmission-line parameters ($x = d$). Generally, we will have three boundary conditions to solve, and three unknown fields [$a_{\text{in}}^c(\omega)$, $a_{\text{out}}^c(\omega)$ and $a_{\text{out}}^f(\omega)$]. The requirements of a continuous voltage distribution and current conservation across $x = d$ imply the linear conditions

$$\Phi(d^-, t) = \Phi(d^+, t), \quad (9)$$

$$\frac{\partial \Phi(d^-, t)}{L_0 \partial x} = \frac{\partial \Phi(d^+, t)}{L_1 \partial x}. \quad (10)$$

These can be solved by the Fourier transformation.

The main challenge is to solve the boundary condition at the junction, where current conservation gives a nonlinear and time-dependent condition

$$C_J \ddot{\Phi}(0, t) + \frac{1}{L_0} \frac{\partial \Phi(x, t)}{\partial x} \Big|_{x=0} = -I_c \sin \left[\frac{2\pi}{\Phi_0} \Phi(0, t) - \omega_J t \right]. \quad (11)$$

Here, $I_c = (2\pi/\Phi_0) E_J$ is the junction's critical current and $\omega_J = 2eV/\hbar$ is the Josephson frequency. Classically, for $Z_0 = Z_1$ and $T = 0$ (no input), this is equivalent to a resistively and capacitively shunted junction (RCSJ) model of a JJ [14].

3. Perturbative input–output approach

We want to derive a solution for the outgoing free-space field, $a_{\text{out}}^{\text{f}}(\omega)$, as a function of the incoming field in the same region, $a_{\text{in}}^{\text{f}}(\omega)$. The challenge is that the boundary condition at the junction is highly nonlinear, containing all moments of the field operators $a_{\text{in/out}}^{\text{c}}(\omega)$ and $[a_{\text{in/out}}^{\text{c}}(\omega)]^\dagger$. A linearization of this condition, performed in appendix A, captures some of the essential physics, but is limited to the second order in the photonic processes and does not, for example, describe correctly the effect of low-frequency phase fluctuations. In the case of a weakly damped resonator ($Z_1 \gg Z_0$), a single cavity mode can also be picked out and be described as a damped oscillator [9, 10], but with a limited description of the important low-frequency modes. Here, we use a different approach and derive a solution for the continuous-mode output field operators as a power series in the junction’s critical current I_c .

3.1. Unperturbed solution

The starting point is the solution for $I_c = 0$, i.e. when the Cooper-pair tunneling is neglected. By a Fourier transformation (appendix B) we obtain the linear dependence

$$a_{\text{out}}^{\text{f}}(\omega) = R(\omega)a_{\text{in}}^{\text{f}}(\omega), \quad (12)$$

$$R(\omega) = \frac{1 + r e^{-2ik_{\omega}^{\text{c}}d - i\theta(\omega)}}{e^{-i\theta(\omega)} + r e^{2ik_{\omega}^{\text{c}}d}}.$$

Here $e^{i\theta(\omega)} = C^*(\omega)/C(\omega)$, $C(\omega) = 1 + iZ_1C_J\omega$ and $r = (Z_1 - Z_0)/(Z_0 + Z_1)$. Similarly, we can solve for the cavity out-field $a_{\text{out}}^{\text{c}}(\omega)$ as a function of the free-space input $a_{\text{in}}^{\text{f}}(\omega)$,

$$a_{\text{out}}^{\text{c}}(\omega) = A(\omega)a_{\text{in}}^{\text{f}}(\omega), \quad (13)$$

$$A(\omega) = \frac{2\sqrt{\frac{Z_1}{Z_0}}e^{-2ik_{\omega}^{\text{c}}d}}{\left(1 + \frac{Z_1}{Z_0}\right)e^{-2ik_{\omega}^{\text{c}}d - i\theta(\omega)} + \frac{Z_1}{Z_0} - 1},$$

where $A(\omega)$ gives the response of the cavity to an external drive and possesses information of its resonance frequencies. With the help of this, the operator for the phase difference at the junction, $\phi_0(t) \equiv 2\pi\Phi(0, t)/\Phi_0$, can be written

$$\phi_0(t) = \frac{\sqrt{4\pi\hbar Z_1}}{\Phi_0} \int_0^\infty \frac{d\omega}{\sqrt{\omega}} \bar{A}(\omega)a_{\text{in}}^{\text{f}}(\omega)e^{-i\omega t} + \text{h.c.} \quad (14)$$

Here, $\bar{A}(\omega) = A(\omega)/C^*(\omega)$ and we also note the useful relation $R(\omega) = \bar{A}(\omega)/\bar{A}^*(\omega)$. The corresponding phase fluctuations are equivalent to that of the ‘tunneling’ impedance $Z_t(\omega)$ [2], defined as

$$\text{Re}[Z_t(\omega)] \equiv Z_1|\bar{A}(\omega)|^2, \quad (15)$$

$$\langle \phi_0(t)\phi_0(t') \rangle = 2 \int_{-\infty}^\infty \frac{d\omega}{\omega} \frac{\text{Re}[Z_t(\omega)]}{R_Q} \frac{e^{-i\omega(t-t')}}{1 - e^{-\beta\hbar\omega}},$$

where $R_Q = h/4e^2$ is the (superconducting) resistance quantum. In the ensemble average we assume thermal equilibrium for the incoming free-space modes, used throughout this paper. For the open line ($Z_0 = Z_1$) case, the impedance (15) describes a capacitor C_J and a resistor Z_0 in parallel, whereas for the cavity case ($Z_1 \gg Z_0$) it describes a capacitively shunted $\lambda/4$ -resonator, with resonances approximately at $\omega_k = (2k + 1)\omega_0$, where $\omega_0 = \pi/2d\sqrt{C_1L_1}$ and $k \in [0, 1, 2, \dots]$.

3.2. First- and second-order solutions

To seek a solution that includes Cooper-pair tunneling ($I_c \neq 0$), we multiply the right-hand side of the boundary condition (11) by a formal dimensionless parameter ξ , and correspondingly write the solution for the annihilation operators of the outgoing field in the open space as $a_{\text{out}}^f(\omega) = \sum_{n=0}^{\infty} \xi^n a_n(\omega)$. The zeroth-order solution, $a_0(\omega)$, corresponds to $I_c = 0$ and was obtained in (12). We make a similar expansion for the fields inside the cavity and for the phase difference across the JJ. The input field in the free space, $a_{\text{in}}^f(\omega)$, is independent of ξ , as the output in this region does not reflect back. The task is to find the other fields as a function of the known input, $a_{\text{in}}^f(\omega)$, for small $I_c \neq 0$.

We solve the boundary condition at the junction order by order in ξ . By a straightforward calculation we find the leading-order solution (appendix B)

$$a_1^f(\omega) = iI_c \sqrt{\frac{Z_1}{\hbar\omega\pi}} \bar{A}(\omega) \int_{-\infty}^{\infty} dt e^{i\omega t} \sin[\phi_0(t) - \omega_J t]. \quad (16)$$

We observe that the operator is a (sinusoidal) function of the zeroth-order phase difference operator (14). In the second order for ξ (and I_c) we obtain

$$a_2^f(\omega) = iI_c \sqrt{\frac{Z_1}{\hbar\omega\pi}} \bar{A}(\omega) \int_{-\infty}^{\infty} dt e^{i\omega t} [\sin[\phi_0(t) - \omega_J t], z(t)]. \quad (17)$$

Here, the operator $z(t)$ ($\propto I_c$) is a solution to the equation $\phi_1(t) = [\phi_0(t), z(t)]$, where ϕ_1 is the phase-difference operator in first order, obtained via the leading-order solution (16), see appendix B. Important here is that the operators $\phi_i(t)$ do not commute with each other.

Thus, we have obtained a solution for (11) to second order in ξ as a function of the operator $z(t)$, which still needs to be solved. In the case of semi-infinite transmission line ($Z_0 = Z_1$), we find a simple explicit form of $z(t)$,

$$z(t) = -i \frac{E_J}{2\hbar} \int_{-\infty}^{\infty} dt' \left[1 + \frac{\text{Sgn}(t-t')}{e^{\omega_c|t-t'|} - 1} \right] \cos[\phi_0(t') - \omega_J t'].$$

Here, $\omega_c = 1/Z_0 C_J$. The solution has an apparent divergence at $t = t'$, which cancels for symmetry reasons in all measurable quantities discussed in this paper. We observe that the operator $z(t)$ is also a trigonometric function of the zeroth-order phase-difference operator. Also generally ($Z_0 \neq Z_1$), $z(t)$ has the form $\int_{-\infty}^{\infty} dt' \mathcal{S}(t-t') \cos[\phi_0(t') - \omega_J t']$, where $\mathcal{S}(t-t')$ is a scalar function. The trigonometric functions can be decomposed into exponential operators $e^{\pm i[\phi_0(t) - \omega_J t]}$, that correspond to charge transfers of $2e$ across the JJ in the two possible directions. [2] Thus, we see that the solutions (16), (17) include all possible tunneling processes up to the second order.

We can now study the consistency of our solution, by checking if the output radiation field satisfies the commutation relation (8). This property is vital as, for example, it secures causality

in the theory [13]. We obtain up to second order

$$\begin{aligned} \left[a_{\text{out}}^{\text{f}}(\omega), [a_{\text{out}}^{\text{f}}(\omega')]^{\dagger} \right] &= |R(\omega)|^2 \delta(\omega - \omega') + \xi \left([a_1(\omega), a_0^{\dagger}(\omega')] + [a_0(\omega), a_1^{\dagger}(\omega')] \right) \\ &+ \xi^2 \left([a_2(\omega), a_0^{\dagger}(\omega')] + [a_0(\omega), a_2^{\dagger}(\omega')] + [a_1(\omega), a_1^{\dagger}(\omega')] \right), \end{aligned} \quad (18)$$

using the input field commutation relation $[a_{\text{in}}^{\text{f}}(\omega), [a_{\text{in}}^{\text{f}}(\omega')]^{\dagger}] = \delta(\omega - \omega')$. Since $|R(\omega)| = 1$, the first term on the right-hand side produces the desired δ -function. A straightforward calculation (appendix B) shows that the rest of the terms, order by order in ξ , sum to zero. This confirms that the commutation relation is indeed valid, up to the order our solution allows us to check this.

4. Emission characteristics I: photon-flux density

Thus, having derived explicit expressions for the outgoing field-operators to second order in the junction's critical current, we go on to study properties of the output radiation. We first investigate general relations for the amplitude correlations, and after this consider their explicit forms. The truncation of the power series to leading order can be made for small transparency JJs, i.e. for small I_c . The exact definition of 'small' is then addressed in section 4.4. In later parts of the paper, sections 5 and 6, we discuss results of similar calculations but done for higher-order correlations.

4.1. General properties for the amplitude correlations

By a direct calculation, we obtain for the amplitude correlations related to the photon-flux and power-spectral densities

$$\langle a_{\text{out}}^{\dagger}(\omega) a_{\text{out}}(\omega') \rangle = 2\pi f(\omega) \delta(\omega - \omega'). \quad (19)$$

We use here the notation $a_{\text{out}}(\omega) \equiv a_{\text{out}}^{\text{f}}(\omega)$. The function $f(\omega)$ is identified as the photon-flux density [15]. This diagonal form is a result of the finite phase-coherence time, present already in the zeroth-order phase-difference (14). The phase difference performs a quantum Brownian motion in time, [16] and it follows that expectation values of type $\langle e^{i\phi_0(t)} e^{i\phi_0(t')} \rangle$ are zero. This also implies that the amplitude correlations related to possible squeezing are zero

$$\langle a_{\text{out}}(\omega) a_{\text{out}}(\omega') \rangle = 0. \quad (20)$$

In general, due to the random phase fluctuations there is on average no phase coherence in the output radiation. Further, only even powers of the critical current are present in the power series of the photon-flux density, or of any higher-order correlator considered in this paper,

$$f(\omega) = \sum_{n=0}^{\infty} I_c^{2n} \mathcal{F}_n(\omega), \quad (21)$$

where functions $\mathcal{F}_n(\omega)$ are independent of I_c . This follows again from the phase fluctuations, namely because $\langle \prod_m e^{\pm i\phi_0(t_m)} \rangle = 0$, for odd integers m .

We further divide the leading-order result for the output photon-flux-density, (19), as

$$f(\omega) = f_{\text{t}}(\omega) + f_{\text{th}}(\omega). \quad (22)$$

Here the term $f_i(\omega)$ is the photon-flux density created by inelastic Cooper-pair tunneling, and the part $f_{\text{th}}(\omega)$ describes reflection of the incoming thermal photons, being finite only for $T \neq 0$. In the following we consider the explicit forms of $f_i(\omega)$ and $f_{\text{th}}(\omega)$.

4.2. Emission from inelastic Cooper-pair tunneling $f_i(\omega)$

Radiation due to inelastic Cooper-pair tunneling is obtained by inserting the leading-order solution for both operators $a_{\text{out}}^{(\dagger)}$ in (19). A straightforward calculation gives (appendix C),

$$\begin{aligned} f_i(\omega) &= \int_0^\infty d\omega' \frac{1}{2\pi} \langle a_1^\dagger(\omega) a_1(\omega') \rangle \\ &= \frac{I_c^2 \text{Re}[Z_t(\omega)]}{2\omega} [P(\hbar\omega_J - \hbar\omega) + P(-\hbar\omega_J - \hbar\omega)]. \end{aligned} \quad (23)$$

Here, the function $P(E)$ is the probability to exchange energy E with the electromagnetic environment, in this case with the transmission line, defined as

$$P(E) = \frac{1}{2\pi\hbar} \int_{-\infty}^\infty dt e^{J(t) + i\frac{E}{\hbar}t}, \quad (24)$$

where the phase correlator function, $J(t) = \langle [\phi_0(t) - \phi_0(0)]\phi_0(0) \rangle$, is a measure of phase fluctuations in the zeroth order. Equation (23) was obtained first in [6] by applying the theory of inelastic Cooper-pair tunneling [2], i.e. $P(E)$ -theory, and keeping track of the simultaneously emitted photons.

We will now analyze the obtained photon-flux density in more detail and compare it with the classical solution, which consists of continuous radiation at the Josephson frequency ω_J , broadened by low-frequency phase fluctuations. The classical power spectral density, defined as $S(\omega) = \hbar\omega f(\omega)$, has the approximate form [14]

$$S_{\text{cl}}(\omega) = \frac{\hbar I_c^2 \text{Re}[Z_t(\omega_J)]}{2} \frac{1}{\pi} \frac{\Gamma}{\hbar^2(\omega_J - \omega)^2 + \Gamma^2}, \quad (25)$$

where we assume a small $\Gamma = 4\pi k_B T Z_0/R_Q \equiv 2\hbar D$ compared to $\hbar\omega_J$. The same result is obtained also from (23) by inserting phase correlations of classical (thermal) phase diffusion [17], $J(t) = -D|t|$. In particular, for $T = 0$ one has $J(t) = 0$ and $P(E) = \delta(E)$. Then all the radiation is emitted at $\omega = \omega_J$ with the total power $I_c^2 \text{Re}[Z_t(\omega_J)]/2$. In an exact classical solution also higher harmonics and a change in the dc-voltage across the junction exist, but the main picture remains.

In the quantum-mechanical treatment of the EM fields, two qualitative differences appear when $T \rightarrow 0$: (i) the linewidth remains finite due to shot noise in the charge transport [14, 18–24]; and (ii) radiation below ω_J has a finite tail due to multi-photon emission [6, 7]. Whereas property (i) is not captured by the leading-order perturbation theory done here (except for the derivation of the zero-frequency shot noise, see section 4.4), property (ii) is seen as an asymmetric broadening of the $P(E)$ -function. At zero temperature and for $Z_0 = Z_1$, the $P(E)$ -function has an approximate form ($E > 0$) [1, 2],

$$P(E) = \frac{\exp(-2\rho\gamma_E)}{\Gamma(2\rho)} \frac{1}{E} \left[\pi\rho \frac{E}{4E_{C_1}} \right]^{2\rho}, \quad (26)$$

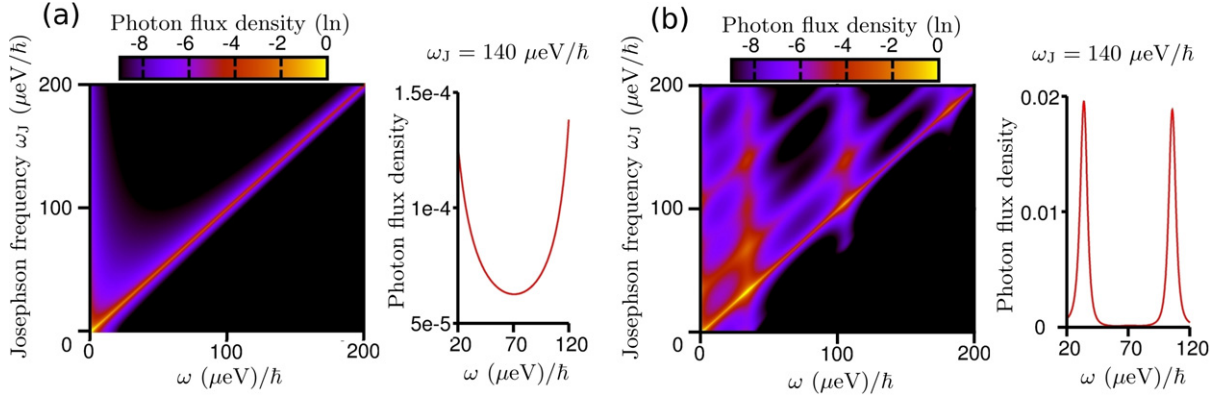


Figure 2. Photon-flux density $f_t(\omega)$ as a function of the Josephson frequency $\omega_J = 2eV/\hbar$ (left panels of (a) and (b)) and for a single value $\omega_J = 140 \mu eV/\hbar$ (right panels). The Josephson radiation is seen as a diagonal resonance $\omega = \omega_J$ in the photon flux density (left panels). The flux is asymmetric around the diagonal, as for $\omega > \omega_J$ the emission is suppressed by the temperature, but for $\omega < \omega_J$ multi-photon production results in extra emission. When the pair production of photons dominates, the photon flux becomes symmetric around half of the Josephson frequency ω_J , as seen for the single picked value $\omega_J = 140 \mu eV/\hbar$ (right panels). In (b) this is approximately the sum of the two resonance frequencies in the cavity, and emission to these modes is enhanced. We use $E_J = 15 \mu eV$, $C = 10$ fF, $T = 100$ mK, $Z_0 = 100 \Omega$, (a) $Z_1 = 100 \Omega$ or (b) $Z_1 = 500 \Omega$ with $f_0 = 1/4d\sqrt{C_1 L_1} = 10$ GHz.

where γ_E is the Euler constant, $E_{C_j} = e^2/2C_j$ is the junction charging energy and $\rho = Z_0/R_Q$ is the dimensionless resistance of the transmission line. For $E < 0$ one has $P(E) = 0$, i.e. no energy can be extracted from the environment.

The result (26) is obtained by using [1, 16, 25] $J(t) = -2\rho [\ln(\omega_R|t|) + \gamma + i\frac{\pi}{2}\text{sign}(t)]$. This zero temperature long-time behavior is a good approximation also at finite temperatures for frequencies $\omega < \omega_J - k_B T/\hbar$. For a typical low-Ohmic transmission line, $\rho \ll 1$, the resulting power density is peaked at the Josephson frequency ω_J with the magnitude $\sim I_C^2 Z_0 \delta(\omega_J - \omega)/2$. A finite tail extends to lower frequencies, $\omega < \omega_J - k_B T/\hbar$, with the form

$$f_t(\omega) \approx I_C^2 Z_0 \frac{\rho}{\hbar \omega (\omega_J - \omega)}. \quad (27)$$

This is symmetric around half the Josephson frequency, $\omega_J/2$, indicating that the radiation results from photons created in pairs [7] whose frequencies ω_a and ω_b add up to the Josephson frequency ω_J . This result can be derived also by straight linearization of the boundary condition, which includes maximally two photon emission processes, as demonstrated in appendix A. Similar results hold also for the cavity configuration, $Z_1 > Z_0$. In particular, if the Josephson frequency matches the sum of the frequency of two modes, strong pair production to these modes is observed. Numerical results for the photon-flux density for the free-space and cavity configurations are presented in figure 2.

4.3. Elastic and inelastic reflection of thermal photons, $f_{th}(\omega)$

In addition to the radiation created by inelastic Cooper-pair tunneling, the leading-order result (22) has a term proportional to the Bose factor, which we further divide as

$f_{\text{th}}(\omega) = f_0(\omega) + f_{\text{in}}(\omega)$. The part $f_0(\omega)$ describes the zeroth-order (elastic) reflection of photons at the junction

$$f_0(\omega) \equiv \int_0^\infty d\omega' \frac{1}{2\pi} \left\langle a_0^\dagger(\omega) a_0(\omega') \right\rangle = \frac{1}{2\pi} \frac{1}{e^{\beta\hbar\omega} - 1}. \quad (28)$$

The inelastic term $f_{\text{in}}(\omega)$ comes from correlators between the zeroth- and second-order operators. For the free-space configuration, $Z_0 = Z_1$, we obtain (appendix C)

$$f_{\text{in}}(\omega) = \frac{1}{e^{\beta\hbar\omega} - 1} \frac{I_c^2 \text{Re}[Z_t(\omega)]}{2\omega} \sum_{\pm} [P(\pm\hbar\omega_J - \hbar\omega) - P(\pm\hbar\omega_J + \hbar\omega)]. \quad (29)$$

We interpret this as an inelastic reflection of thermal photons, exchanging energy with a Cooper-pair tunneling in either direction. The term proportional to $P(\pm\hbar\omega_J - \hbar\omega)$ contributes as photon emission to the frequency ω , and the term $\propto P(\pm\hbar\omega_J + \hbar\omega)$ as photon absorption from this frequency. Such processes do not contribute to the net current, and are a small correction to $f_t(\omega)$ for the situations considered in this paper.

4.4. Convergence

So far we have found that it is the phase fluctuations across the JJ that describe Cooper-pair tunneling and simultaneous photon emission in the leading order. To study the convergence of the perturbation expansion, we then investigate the spectrum of the phase fluctuations at the junction. In particular, we compare the magnitude of the zeroth-order contribution with the magnitude of the leading-order contribution. For a rapidly converging perturbation expansion, the latter should be much smaller than the first. This should hold for all frequencies, since the right-hand side of the boundary condition at the junction (11), mixes all combinations of frequency terms summing up to ω_J . This leads to the comparison

$$4\text{Re}[Z_t(\omega)] \langle a_0^\dagger a_0 + a_0 a_0^\dagger \rangle \gg \text{Re}[Z_f(\omega)] \langle a_1^\dagger a_1 + a_1 a_1^\dagger \rangle. \quad (30)$$

Here we have defined $\text{Re}[Z_f(\omega)] = Z_1 |\kappa_+ + \kappa_- e^{2ik_\omega^c d}|^2$, where $\kappa_{\pm} = (\sqrt{Z_0/Z_1} \pm \sqrt{Z_1/Z_0})/2$. This leads us to the general condition

$$\frac{2}{\pi} \coth\left(\frac{\beta\hbar\omega}{2}\right) \gg \frac{I_c^2}{2\omega} \text{Re}[Z_f(\omega)] \sum_{\pm\pm} [P(\pm\hbar\omega_J \pm \hbar\omega)]. \quad (31)$$

This is a relation for the smallness of the junction's critical current I_c . For frequencies below the cut-off frequency ω_c , $\text{Re}[Z_f(\omega)]$ is approximately equal to $\text{Re}[Z_t(\omega)]$, and in the following we will replace $Z_f(\omega)$ by $Z_t(\omega)$. We now examine the condition (31) explicitly at zero frequency, at the Josephson frequency, and then finally for frequencies between these special frequencies.

Let us investigate the zero-frequency limit by multiplying each side of (31) by $\hbar\omega$. We obtain

$$\frac{4k_B T}{\pi} \gg \hbar I_c^2 \text{Re}[Z_t(0)] [P(\hbar\omega_J) + P(-\hbar\omega_J)]. \quad (32)$$

Using the leading-order result for the simultaneous electric current $I = I_c \langle \sin[\phi(t) - \omega_J t] \rangle = I^+ - I^-$, where $I^\pm(V) = (\pi\hbar I_c^2/4e) P(\pm\hbar\omega_J)$, we obtain the relation

$$\frac{4k_B T}{\text{Re}[Z_t(0)]} \gg 4e [I^+(V) + I^-(V)]. \quad (33)$$

This compares Johnson–Nyquist current noise (left-hand side) with the shot-noise coming from the charge transport (right-hand side), the noise considered also in [14, 18–24]. For an Ohmic impedance ($Z_0 = Z_1$) this implies

$$k_B T \gg \pi^2 \rho^2 \frac{E_J}{2eV} E_J. \quad (34)$$

The second condition is calculated at the Josephson frequency $\omega = \omega_J$. The contribution from ω_J would act back to the low-frequency spectrum in the next perturbation round and would affect, for example, a possible shift in the average voltage across the junction. Analysis at the Josephson frequency gives us

$$4k_B T \gg \hbar I_c^2 \frac{\text{Re}[Z_t(\omega_J)]}{2eV} \frac{R_Q}{2\pi \text{Re}[Z_t(0)]}. \quad (35)$$

To derive this, we have used the approximation $P(0) \approx (1/\Gamma\pi)$. We assume now that the Josephson frequency does not match with a resonance frequency in the cavity (but it still can match a sum of two). We have then $\text{Re}[Z_t(\omega_J)] \approx \text{Re}[Z_t(0)]$, and we obtain the condition

$$4k_B T \gg \frac{E_J}{2eV} E_J. \quad (36)$$

For an Ohmic impedance this is usually slightly more strict as (34), as typically $\rho \sim 1/20 > 1/2\pi$. It is also independent of Z_0 . For the Ohmic case this can then be converted to a demand that thermal dephasing has to be faster than inelastic Cooper-pair tunneling, since $D \gg I(V)/2e$ is equivalent to $2k_B T \gg E_J^2/2eV$ (under the approximation $P(\hbar\omega) \approx 2\rho/\hbar\omega$). However, if the Josephson frequency is exactly at the resonance, we obtain

$$4k_B T \gg \frac{E_J}{2eV} E_J Q_0^2. \quad (37)$$

Here we have used the result for the Q -factors of the resonance modes $Q_n = (2n+1)\pi Z_1/4Z_0$ ($n = 0, 1, 2, \dots$).

For the analysis at the middle frequencies $k_B T/\hbar < \omega < \omega_J - k_B T/\hbar$ we consider the approximation $P(\hbar\omega) \approx 2Z_t(\omega)/R_Q\hbar\omega$, which gives

$$1 \gg \frac{eI_c Z_t(\omega)}{\hbar\omega} \frac{eI_c Z_t(\omega_J - \omega)}{\hbar(\omega_J - \omega)}. \quad (38)$$

For a resonant environment this sets a limit between the critical current and the sharpness (Q -factor) of the mode. One then gets the condition $I_c Z_1 Q_0 \ll V$. For an Ohmic impedance we obtain the condition $I_c Z_0 \ll V$, a known convergence condition for the higher orders of $P(E)$ -theory obtained in [24].

5. Emission characteristics II: second-order coherence

To study statistics of the emitted photons in more detail, we investigate the second-order coherence $G^{(2)}(\tau)$ for the output radiation, i.e. the probability to detect a pair of photons with time interval τ . The possibility for multi-photon emission implies bunching of the outgoing photons, meaning an increased probability of detecting photon pairs simultaneously. In this section, we consider our results for $G^{(2)}(\tau)$, obtained by including the leading contributions up to the fourth order in the critical current I_c .

5.1. Photon coherences

We start with the first-order coherence, $G^{(1)}(\tau)$, for a continuous-mode field defined as [26]

$$G^{(1)}(\tau) \equiv \frac{\hbar Z_0}{4\pi} \int_0^\infty d\omega d\omega' \sqrt{\omega\omega'} \langle a_{\text{out}}^\dagger(\omega) a_{\text{out}}(\omega') \rangle e^{i\omega\tau}.$$

Here we use the notation $\int_0^\infty d\omega d\omega' \equiv \int_0^\infty d\omega \int_0^\infty d\omega'$. Similarly as before, we estimate this up to second order in I_c . We can relate this to the photon-flux density, equation (22), and obtain

$$G^{(1)}(\tau) = \frac{\hbar Z_0}{2} \int_0^\infty d\omega \omega [f_t(\omega) + f_{\text{th}}(\omega)] e^{i\omega\tau}.$$

In the following, we are interested in the contribution due to an inelastic Cooper-pair tunneling, $f_t(\omega)$,

$$G_t^{(1)}(\tau) = \frac{I_c^2 Z_0}{4} \int_0^\infty \hbar d\omega e^{i\omega\tau} \text{Re}[Z_t(\omega)] P(\hbar\omega_J - \hbar\omega). \quad (39)$$

Here, we have neglected the vanishing contribution due to backward Cooper-pair tunneling, $\propto P(-\hbar\omega_J - \hbar\omega)$.

The second-order coherence gives information on correlations between the emitted photons. This is defined for a continuous-mode field as [26]

$$G^{(2)}(\tau) \equiv \left(\frac{\hbar Z_0}{4\pi}\right)^2 \int_0^\infty d\omega d\omega' d\omega'' d\omega''' \sqrt{\omega\omega'\omega''\omega'''} e^{i\tau(\omega' - \omega'')} \langle a_{\text{out}}^\dagger(\omega) a_{\text{out}}^\dagger(\omega') a_{\text{out}}(\omega'') a_{\text{out}}(\omega''') \rangle. \quad (40)$$

The leading-order contribution for (40) comes again from the second order in I_c , which describes the effect of single-Cooper-pair tunneling. To obtain analytical results we calculate $G_t^{(2)}(\tau)$ for the JJ connected directly to the free space, $Z_0 = Z_1$, at very low temperatures (for a more general expression see appendix D). After a straightforward calculation we obtain

$$G_t^{(2)}(\tau) = \left(\frac{I_c^2 Z_0^2}{4}\right)^2 \left(\frac{1}{\pi E_J}\right)^2 \int_0^\infty \hbar ds \left(\frac{2\hbar}{\tau}\right)^2 \sin^2\left(\frac{\tau s}{2}\right) P[\hbar(\omega_J - s)]. \quad (41)$$

Here, we have neglected terms proportional to the Bose factor, i.e. $\propto f_0(\omega)$. In the following, we use this result to study photon bunching in the output radiation.

5.2. Bunching

An important quantity describing photon emission is the relation between the first- and second-order coherences

$$g^{(2)}(\tau) = \frac{G^{(2)}(\tau)}{[G^{(1)}(0)]^2}. \quad (42)$$

This basically compares probabilities for single- and two-photon detection. If $g^{(2)}(0) < 1$, the field is called antibunched, and if $g^{(2)}(0) > 1$ the field is bunched. For a Poissonian process the result is $g^{(2)}(0) = 1$, while for thermal radiation $g^{(2)}(0) = 2$. Arbitrarily high bunching is possible also classically whereas antibunching is a pure sign of nonclassicality [26].

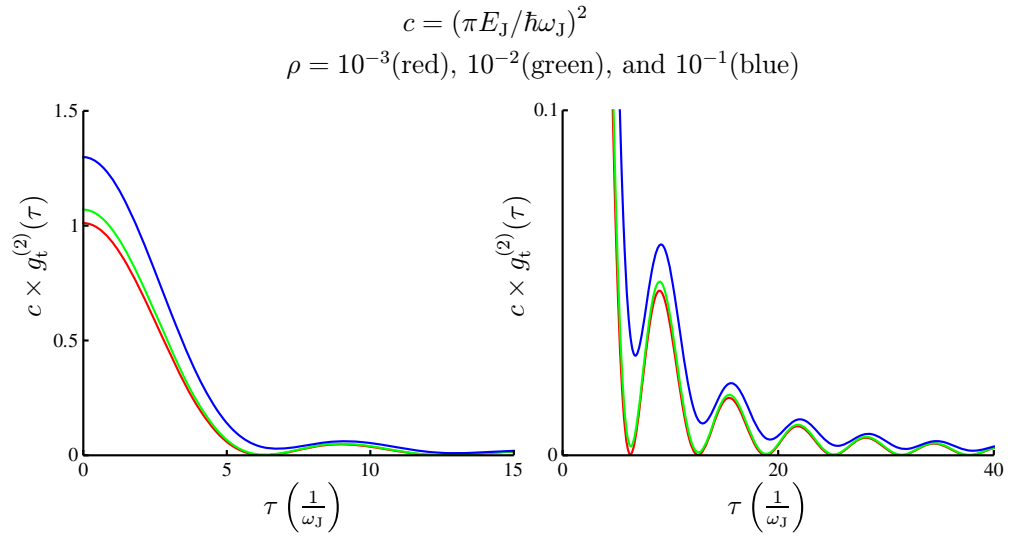


Figure 3. The normalized second-order coherence for a JJ connected directly to the free space, as estimated from (39) and (41) using the $P(E)$ -function (26). We use here $\rho = 10^{-3}$, 10^{-2} and 10^{-1} , from bottom to top, and we have chosen $E_C = \hbar \omega_J$. We see that the bunching, $g_t^{(2)}(0)$, is close to the estimate (43) when $\rho \ll 1$. The second-order coherence decays due to finite bandwidth, and has an analogous form to the intensity pattern in single-slit diffraction.

With the analytical values of the first- and the second-order coherences we can immediately get an estimate for the bunching in the free-space configuration ($Z_0 = Z_1$). We consider a typical transmission line ($\rho \ll 1$, $\omega_J \ll \omega_c$) and solution (26), and obtain (appendix D)

$$g_t^{(2)}(0) = \frac{G_t^{(2)}(0)}{[G_t^{(1)}(0)]^2} \approx \left(\frac{\hbar \omega_J}{\pi E_J} \right)^2. \quad (43)$$

This can be made arbitrarily high by decreasing the critical current, i.e. the emitted power. This property is typical for pair production of photons. Notably, result (43) is independent of ρ , even though the power is proportional to ρ . In figure 3, we visualize the time dependence of $g_t^{(2)}(\tau)$.

As Cooper-pair tunneling is also accompanied by an emission of low-energy photons, describing a simultaneous change in the voltage across the junction, it is clearer for the interpretation of the results not to include frequencies in the neighborhood of $\omega = 0$ or ω_J . We consider then a small interval $\Delta\omega$ of frequencies around half the Josephson frequency $\omega_J/2$, i.e. $\omega_J/2 - \Delta\omega/2 < \omega < \omega_J/2 + \Delta\omega/2$, which in an experiment corresponds to a filtering of the output radiation [27]. One obtains for the corresponding second-order coherence (appendix D)

$$G_t^{(2)}(0) \approx \left(\frac{I_c^2 Z_0^2}{4} \right)^2 \left(\frac{\hbar \Delta\omega}{\pi E_J} \right)^2.$$

The related first-order coherence, within the same approximation, is $G_t^{(1)}(0) \approx \rho I_c^2 Z_0^2 \Delta\omega / \omega_J$. Therefore, we obtain the bunching, if measured in a small frequency interval around $\omega_J/2$,

$$g_t^{(2)}(0) \approx \left(\frac{1}{4\rho} \right)^2 \left(\frac{\hbar \omega_J}{\pi E_J} \right)^2. \quad (44)$$

This is proportional to $1/\rho^2$, and for the considered case of small ρ , is much larger than result (43) for the complete output field.

If we consider detection in a small frequency interval completely above half the Josephson frequency $\omega_J/2$, we obtain the leading-order result $g_t^{(2)}(0) \approx 0$ (appendix D), and exactly zero at the zero temperature. This is because the photon production at these frequencies occurs through multi-photon processes, and the emission of two (or more) photons above $\omega_J/2$ is not possible from a single-Cooper-pair process. However, the result $g_t^{(2)}(0) = 0$ does not imply that the field is antibunched, since contributions from higher orders are neglected. The next-order contribution for $G_t^{(2)}(0)$ comes from the fourth order, which has a special meaning as this is also the leading order of $|G_t^{(1)}(0)|^2$. This order is also the first one to describe photon emission from two Cooper-pair tunnelings. Analytical results can be obtained for the Ohmic environment in the considered case $\rho \ll 1$. The most important contribution comes from a term describing two photon emission processes due to two (correlated) Cooper-pair tunnelings, $\langle a_1^\dagger a_1^\dagger a_1 a_1 \rangle$. For small ρ and approximation $J(t) = -D|t| - i\pi\rho \text{Sgn}(t)$ [17], we get through a lengthy analytical calculation a contribution $g_t^{(2)}(0) = 2 - \bar{B}$, where for $\rho \ll 1$ and a bandwidth larger than thermal dephasing D , we obtain $\bar{B} \approx 1$. This implies that the photon emission at these frequencies ($\omega_J/2 < \omega \ll \omega_J$) and for $\rho \ll 1$ is close to a Poissonian process.

6. Nonclassicality

The electromagnetic field is nonclassical if it cannot be described by the classical theory of electromagnetism. One example is a quadrature squeezed state of single mode, for which the width of the Wigner quasiprobability distribution in one of the quadratures is smaller than the width of a coherent state, i.e. the quantum description of a classical coherent signal [28]. The quadrature squeezing is measured through amplitude auto- and cross-correlations, which are phase-sensitive quantities. In our system, the JJ is driven by a dc voltage, which suffers from both thermal and transport noise. As we will see, this leads to a rather short phase coherence time and no steady-state squeezing. There exists however a number of other relations, that are satisfied by a classical field, but can be violated by a general quantum mechanical field [29]. These are useful in our system, if they are immune to dephasing. An example of such a nonclassicality test is the Cauchy–Schwarz inequality for intensity auto- and cross-correlations, that is known to be violated maximally for a field created through parametric down conversion [28].

In this section, we first address the question of quadrature squeezing in the output radiation, and then go on to derive a Cauchy–Schwarz inequality for photon-flux correlations in the leading-order approximation, which we find to be an optimal way of detecting nonclassicality in the considered system.

6.1. Quadrature squeezing and dephasing

The pair production of photons implies quadrature squeezing [28], which is characterized by correlators of type $\langle a_{\text{out}}(\omega)a_{\text{out}}(\omega') \rangle$. The result (20), however, means that such nonclassical correlations do not exist on average, due to dephasing of the phase difference across the junction. This can be qualitatively visualized as a diffusion of the angle of quadrature squeezing. The situation is analogous to a parametric down conversion with a nonideal drive [26].

To investigate how long it takes for the squeezing angle to be randomized, if one knows its value (or distribution) at time $t = 0$, we consider the phase-coherence function

$$\langle e^{i\phi_0(t)} e^{-i\phi_0(0)} \rangle = e^{J(t)}. \quad (45)$$

In the long-time limit and for finite temperatures its behavior is defined by the zero-frequency impedance Z_0 , via $J(t) \sim -D|t|$, where $D = 2\pi k_B T \rho / \hbar$. Therefore, we identify D as the dephasing rate of quadrature squeezing. For typical values for the low-frequency impedance $Z_0 = 50 \Omega$ and $T = 20$ mK, one has $1/D \approx 8$ ns. Such dephasing times are therefore a very relevant property of a voltage-driven system, and a challenge for a measurement of phase-dependent system properties.

6.2. Cauchy–Schwarz inequality for intensity cross-correlations

A nonclassicality test that is not affected by phase fluctuations must be of higher order in the operators $a_{\text{out}}^{(\dagger)}$. The logical thing to do is to add two more operators to the ensemble average that characterizes squeezing, $\langle a_{\text{out}} a_{\text{out}} \rangle$. Basically, we have two possibilities to consider, the second-order coherence, of type $\langle a_{\text{out}}^\dagger a_{\text{out}}^\dagger a_{\text{out}} a_{\text{out}} \rangle$, or the intensity correlator, of type $\langle a_{\text{out}}^\dagger a_{\text{out}} a_{\text{out}}^\dagger a_{\text{out}} \rangle$. The second-order coherence was considered in section 5, and was found to reveal a high degree of bunching, as a result of photon pair production. However, only antibunching would be a proof of nonclassicality. Therefore, we will now investigate a nonclassicality condition based on the intensity of cross-correlations. In the countable-mode case, a suitable Cauchy–Schwarz inequality is of the form [29]

$$|\langle a_1^\dagger a_1 a_2^\dagger a_2 \rangle|^2 \leq \langle (a_1^\dagger)^2 a_1^2 \rangle \langle (a_2^\dagger)^2 a_2^2 \rangle. \quad (46)$$

In the following, we apply this condition to the considered continuous-mode case.

In the case of continuum of modes, we practically estimate $G^{(2)}(0)$ over a small frequency range $\Delta\omega$ around ω_1 or ω_2 , and similarly for the corresponding cross correlator. Through a straightforward calculation we obtain for the considered auto-correlator (appendix D)

$$\int_{\omega_a - \Delta\omega/2}^{\omega_a + \Delta\omega/2} d\omega_1 d\omega_2 d\omega_3 d\omega_4 \langle a_1^\dagger a_2^\dagger a_3 a_4 \rangle = \frac{2\pi I_c^2 \Delta\omega^3}{\omega_a^2 R_Q} P [\hbar(\omega_J - 2\omega_a)] [\text{Re}[Z_t(\omega_a)]]^2 + \mathcal{O}(\Delta\omega^4). \quad (47)$$

To keep the notation short we mark here $a_i \equiv a(\omega_i)$. $G^{(2)}(0)$ at ω_a is calculated up to the second order in I_c and similarly for the contribution at ω_b .

On the other hand, the intensity cross-correlations between the two frequencies have the form (when $|\omega_a - \omega_b| > \Delta\omega$)

$$\begin{aligned} & \int_{\omega_a - \Delta\omega/2}^{\omega_a + \Delta\omega/2} d\omega_1 d\omega_2 \int_{\omega_b - \Delta\omega/2}^{\omega_b + \Delta\omega/2} d\omega_3 d\omega_4 \langle a_1^\dagger a_2^\dagger a_3^\dagger a_4 \rangle \\ &= \frac{2\pi I_c^2 \Delta\omega^3}{\omega_a \omega_b R_Q} P [\hbar(\omega_J - \omega_a - \omega_b)] \text{Re}[Z_t(\omega_a)] \text{Re}[Z_t(\omega_b)] + \mathcal{O}(\Delta\omega^4). \end{aligned} \quad (48)$$

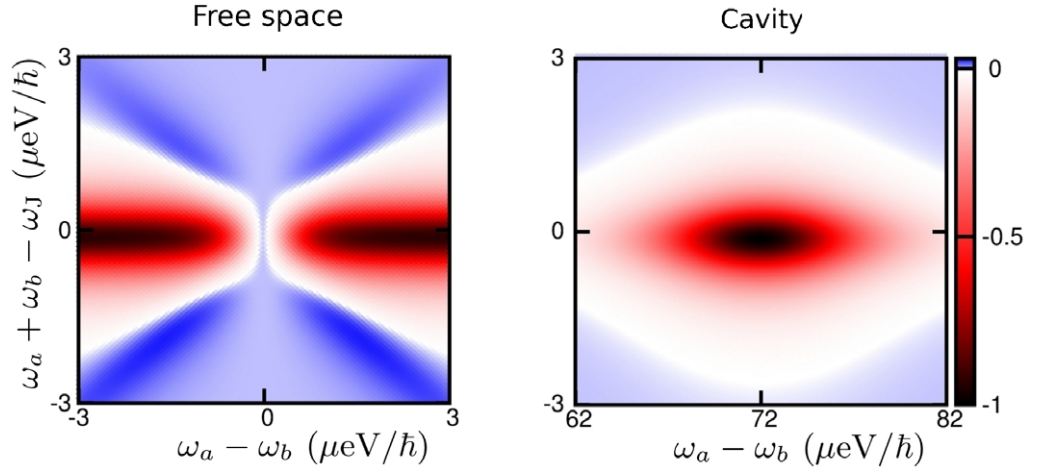


Figure 4. We plot here the violation of the Cauchy–Schwarz inequality (49), $\mathcal{N} = P[\hbar(\omega_J - 2\omega_a)] P[\hbar(\omega_J - 2\omega_b)] - P[\hbar(\omega_J - \omega_a - \omega_b)]^2$, multiplied by the photon-flux densities at the two frequencies, i.e. $\mathcal{N} \times f_i(\omega_a) f_i(\omega_b)$. The color scale is normalized to the maximal value, which is 2×10^5 higher for the cavity configuration (right) compared to the JJ connected directly to free space (left). Negative values are a sign of nonclassicality and the parameters correspond to figure 2. The violation occurs around the condition of photon pair production $\omega_a + \omega_b = \omega_J = 140 \mu eV/\hbar$. For the cavity configuration the observed nonclassicality is enhanced when the two frequencies match the two lowest modes of the cavity, maximizing the photon pair production.

With the results (47) and (48) we obtain then the Cauchy–Schwarz inequality (in the limit $\Delta\omega \rightarrow 0$ and calculated up to second order in I_c)

$$P[\hbar(\omega_J - \omega_a - \omega_b)]^2 \leq P[\hbar(\omega_J - 2\omega_a)] P[\hbar(\omega_J - 2\omega_b)]. \quad (49)$$

This result is valid for both the free-space and the cavity configuration.

The inequality (49) is defined only via the $P(E)$ -function (24). The left-hand side of (49) has a maximum when $\omega_a + \omega_b = \omega_J$, i.e. when the argument goes to zero. If at the same time $|\omega_a - \omega_b| \gg k_B T$, the right-hand side is close to zero, as one of the $P(E)$ -functions has a large negative argument compared to the temperature. In this case the inequality becomes violated, which we visualize in figure 4. The violation is due to nonclassical photon pair production. Generally at $\omega_a = \omega_b$ the nonclassicality cannot be tested with this inequality since the two sides are equal by definition. The use of a resonant environment ($Z_1 \gg Z_0$) does not change the violation of the inequality (49) qualitatively. However, it significantly increases the photon emission rate at certain frequencies, which facilitates experimental detection [7]. As the contribution from thermal radiation is neglected here, the tested frequencies $\omega_{a(b)}$ should be well above $k_B T/\hbar$. Also, in an experiment a detection over a finite bandwidth is used, whose effect should be carefully analyzed.

7. Conclusions and outlook

In conclusion, we have derived a continuous-mode solution for microwave radiation in a transmission line with a dc-voltage bias and which is terminated by a small JJ. This is done

by a perturbative treatment of the boundary condition that describes Cooper-pair tunneling across the JJ. We showed that the method reproduces the previously derived expression for the created photon-flux density, obtained by applying the $P(E)$ -theory. We extended this first by determining the corresponding second-order coherence. We found that the emitted microwave field has a high degree of bunching due to photon pair production at frequencies below the Josephson frequency. We then addressed the question of nonclassicality of the emitted radiation in this region and showed that the photon pair production violates the classical Cauchy–Schwarz inequality for intensity cross-correlations.

The established method opens a possibility for further detailed study of the radiation characteristics in this system. For example, calculations in the higher order access the question of the effect of correlations between consecutive tunneling Cooper pairs. For the considered case of low-Ohmic environment, we obtained bunching in the output radiation. On the other hand, when the transmission-line impedance is increased beyond the resistance quantum, antibunching of the Cooper-pair tunneling is expected, due to the Coulomb blockade [2]. In this regime, the output photons should also be antibunched. Also, summation to all orders can be feasible, if it is known the summation methods for this type of perturbation expansions work. Overall, this system is very rich in physics, covering the limit of dynamical Coulomb blockade at low impedances, to Coulomb blockade in the high-impedance limit. The question of the detailed form and properties of the related output radiation makes this system very interesting for future works. This is motivated also by the technical development towards simultaneous measurements of both microwaves and electrical currents.

Appendix A. Linearization of the boundary condition at the junction

A straightforward way to solve the out-field is to linearize the boundary condition (11) and Fourier transform the problem. The silent assumption is the small fluctuations of the phase difference, $\phi(t)$. This is actually not usually the case, since the (zeroth-order) phase difference performs quantum Brownian motion in time [2, 16]. However, the linearization turns out to give correct results for frequencies $\omega \sim \omega_J/2$ ($\rho \ll 1$), where such fluctuations stay small. This is consistent with the pair production of photons in this frequency range.

In the following we consider linearization in the case of the free-space configuration, $Z_0 = Z_1$, and take the limit $C_J \rightarrow 0$. To do this properly, we rewrite the right-hand side of (11) using the identity

$$\sin[\phi(t) - \omega_J t] = -\cos \phi(t) \sin \omega_J t + \sin \phi(t) \cos \omega_J t.$$

Expanding the right-hand side of this up to linear order in $\phi(t)$, and Fourier transforming, we obtain for this

$$\frac{\pi}{i} [\delta(\omega - \omega_J) - \delta(\omega + \omega_J)] + \sum_{\pm} \frac{\pi^{3/2}}{\Phi_0} \sqrt{\hbar Z_0} \frac{1}{\sqrt{|\omega \pm \omega_J|}} [a_{\text{in}}(\omega \pm \omega_J) + a_{\text{out}}(\omega \pm \omega_J)].$$

Here, for simplicity, we have introduced negative frequencies as $a(-\omega) \equiv a^\dagger(\omega)$. The first two terms represent radiation at the Josephson frequency ω_J , while the other terms describe mixing of this with an additional photonic process where, for example, ω_J is split into two frequencies.

We continue by solving the corresponding boundary condition

$$a_{\text{out}}(\omega) + i \text{Sgn}(\omega) \frac{Z_0 I_c \pi}{\Phi_0} \sqrt{\frac{1}{\omega}} \sum_{\pm} \frac{a_{\text{out}}(\omega \pm \omega_J)}{\sqrt{|\omega \pm \omega_J|}} = a_{\text{in}}(\omega) - i \text{Sgn}(\omega) \frac{Z_0 I_c \pi}{\Phi_0} \sqrt{\frac{1}{\omega}} \sum_{\pm} \frac{a_{\text{in}}(\omega \pm \omega_J)}{\sqrt{|\omega \pm \omega_J|}}.$$

This can be done by writing the equation into the matrix form

$$M_{\text{out}}(\delta\omega) A_{\text{out}}(\delta\omega) = M_{\text{in}}(\delta\omega) A_{\text{in}}(\delta\omega). \quad (\text{A.1})$$

Here the frequency vector A is constructed as [11]

$$A^T = \{a[-N\omega_J + \delta\omega], \dots, a[N\omega_J + \delta\omega]\},$$

where $|\delta\omega| < \omega_J$. This form is possible since the boundary condition mixes only frequencies differing by ω_J . We also have introduced a cut-off $\Omega = N\omega_J$. The matrices M have diagonals 1 and first nondiagonals (in the n th row) $d^{\pm}[(-N-1+n)\omega_J + \delta\omega]$, where the plus sign corresponds to the term $M_{n,n+1}$ and we have

$$d_{\text{out}}^{\pm}(\omega) = \text{Sgn}(\omega) i\pi \frac{I_c}{\Phi_0} Z_0 \frac{1}{\sqrt{|\omega||\omega \pm \omega_J|}}$$

and $d_{\text{in}} = -d_{\text{out}}$. Equation (A.1) has to be solved generally numerically. For small d approximate analytical solution can be sought with the ansatz

$$a_{\text{out}}(\omega) = a_{\text{in}}(\omega) + S^+(\omega) a_{\text{in}}(\omega + \omega_J) + S^-(\omega) a_{\text{in}}(\omega - \omega_J). \quad (\text{A.2})$$

We then find a solution in the lowest order for I_c

$$S^{\pm}(\omega) = -2d^{\pm}(\omega). \quad (\text{A.3})$$

We can now estimate the photon flux density below the Josephson frequency. Using (A.3) one gets for $\omega < \omega_J$ and at $T = 0$

$$f_t(\omega) = \frac{1}{2\pi} |S^-(\omega)|^2 = \frac{\rho I_c^2 Z_0}{\hbar\omega(\omega_J - \omega)}. \quad (\text{A.4})$$

This result is consistent with (27).

Appendix B. Perturbative input–output approach

B.1. Zeroth-order solution

After the Fourier transformation of boundary conditions (9)–(10) we obtain

$$a_{\text{out}}^c(\omega) = \kappa_- a_{\text{in}}^f(\omega) e^{-2ik_{\omega}^c d} + \kappa_+ a_{\text{out}}^f(\omega), \quad (\text{B.1})$$

$$a_{\text{in}}^c(\omega) = \kappa_+ a_{\text{in}}^f(\omega) + \kappa_- a_{\text{out}}^f(\omega) e^{2ik_{\omega}^c d}. \quad (\text{B.2})$$

Here $2\kappa_{\pm} = \sqrt{Z_0/Z_1} \pm \sqrt{Z_1/Z_0}$. Considering the zeroth-order solution, $E_J = 0$, the Fourier transformation ($\omega > 0$) of the boundary condition at the junction, equation (11), gives

$$\mathcal{C}(\omega) a_{\text{out}}^c(\omega) - \mathcal{C}^*(\omega) a_{\text{in}}^c(\omega) = 0. \quad (\text{B.3})$$

The solution is then $a_{\text{out}}^c(\omega) = e^{i\theta(\omega)} a_{\text{in}}^c(\omega)$. Combining this with equations (B.1), (B.2) we obtain (12)–(14).

B.2. Higher-order solution

For higher orders we have no input field from free space and the boundary condition at $x = d$ gets the form ($n \geq 1$)

$$b_n(\omega) = \kappa_+ a_n(\omega), \quad (\text{B.4})$$

$$c_n(\omega) = \kappa_- a_n(\omega) e^{2ik_\omega^c d}. \quad (\text{B.5})$$

Here the output (input) cavity field in the n th order is labeled as b_n (c_n). We rewrite the boundary condition at the junction as

$$b_n(x=0) = c_n(x=0)e^{i\theta(\omega)} + iI_c \frac{\sqrt{Z_1/\hbar\omega\pi}}{\mathcal{C}(\omega)} \int_{-\infty}^{\infty} e^{i\omega t} dt \{\sin[\phi(t) - \omega_J t]\}_{n-1}. \quad (\text{B.6})$$

Here the formal operation $\{\cdot\}_n$ picks out the n th order contribution. It follows then

$$a_n(\omega) = i\sqrt{\frac{Z_1}{\hbar\omega\pi}} \frac{A(\omega)}{\mathcal{C}^*(\omega)} I_c \int_{-\infty}^{\infty} e^{i\omega t} dt \{\sin[\phi(t) - \omega_J t]\}_{n-1}. \quad (\text{B.7})$$

In leading order, we can only include zeroth-order phase difference in the Taylor expansion of operators $e^{\pm i\phi_0 + \xi\phi_1 + \xi^2\phi_2 \dots}$, and we immediately obtain (16). Generally, one can solve the phase difference at the junction in the n th order,

$$\begin{aligned} \phi_n(t) &= \int_0^\infty \frac{d\omega}{\sqrt{\omega}} B(\omega) a_n(\omega) e^{-i\omega t} + \text{h.c.}, \\ B(\omega) &= \frac{\sqrt{\hbar Z_1 \pi}}{\Phi_0} (\kappa_+ + \kappa_- e^{2ik_\omega^c d}). \end{aligned} \quad (\text{B.8})$$

This is self-consistent, since the same order result for $a_n(\omega)$ depends only on the previous order phase-differences.

The phase difference in the leading order has a central role when constructing the general solution. We obtain for this

$$\phi_1(t) = \frac{I_c Z_1}{\Phi_0} \int_{-\infty}^{\infty} dt' \sin[\phi_0(t') - \omega_J t'] \tilde{\mathcal{C}}(t-t'), \quad (\text{B.9})$$

$$\tilde{\mathcal{C}}(t-t') = i \int_0^\infty \frac{d\omega}{\omega} \bar{A}(\omega) (\kappa_+ + \kappa_- e^{2ik_\omega^c d}) e^{-i\omega(t-t')} + \text{h.c.} \quad (\text{B.10})$$

We calculate the explicit form for $Z_0 = Z_1$,

$$\tilde{\mathcal{C}}(t-t') = \pi \left[\text{Sgn}(t-t') \left(1 - e^{-\omega_c |t-t'|} \right) + e^{-\omega_c |t-t'|} \right]. \quad (\text{B.11})$$

B.3. Treatment of $\sin[\phi(t) - \omega_J t]$ to second order

We aim to expand the term $\xi I_c \sin[\phi(t) - \omega_J t]$ to second order in ξ . We have formally $\phi(t) = \phi_0(t) + \xi\phi_1(t) + \dots$, and we need to properly expand the functions

$$e^{\pm i[\phi_0(t) + \xi\phi_1(t) + \xi^2\phi_2(t) + \dots - \omega_J t]} \quad (\text{B.12})$$

to first order in ξ . We know that up to the first order in ξ we can include only operators $\phi_0(t)$ and $\xi\phi_1(t)$ in the Taylor expansion. Therefore we can put $\phi(t) = \phi_0(t) + \xi\phi_1(t)$. We now define

an operator $z(t)$ through the relation $\phi_1(t) = [\phi_0(t), z(t)]$. Through a direct calculation of the Taylor expansion one gets for the first-order contribution

$$\left\{ e^{\pm i[\phi_0(t) + i\xi\phi_1(t)]} \right\}_1 = \xi [e^{\pm i\phi_0(t)}, z(t)]. \quad (\text{B.13})$$

To solve z , we first evaluate commutator $C(t - t') = [\phi_0(t), \phi_0(t')]$. Generally

$$C(t - t') = -4i \int_0^\infty d\omega \frac{\sin \omega(t - t')}{\omega} \frac{\text{Re}[Z_t(\omega)]}{R_Q}. \quad (\text{B.14})$$

We obtain for the special case $Z_0 = Z_1$,

$$C(t - t') = -i \frac{2\pi Z_0}{R_Q} \text{Sgn}(t - t') \left(1 - e^{-\omega_c|t-t'|} \right). \quad (\text{B.15})$$

We then investigate the commutator

$$[\phi_0(t), \cos[\phi_0(t') - \omega_J t']] = -C(t - t') \sin[\phi_0(t') - \omega_J t'].$$

Here we have used that $[\phi_0(t), e^{\pm i\phi_0(t')}] = \pm iC(t - t') e^{\pm i\phi_0(t')}$. Comparing this with solution (B.8) we deduce

$$z(t) = -\frac{I_c Z_1}{\Phi_0} \int_{-\infty}^\infty dt' \cos[\phi_0(t') - \omega_J t'] \frac{\tilde{C}(t - t')}{C(t - t')}. \quad (\text{B.16})$$

For the open-space configuration ($Z_0 = Z_1$) we then get

$$\frac{\tilde{C}(t)}{C(t)} = i \frac{R_Q}{2Z_0} \left[1 + \frac{\text{Sgn}(t)}{e^{\omega_c|t|} - 1} \right], \quad (\text{B.17})$$

which leads to (17). This expansion (with methods shown in appendix C) can also be used to rederive the $P(E)$ -theory net current across the JJ, used in section 4.4.

B.4. Commutation relations for the out field

We express the zeroth-order solution in the form

$$a_{\text{out}}^0(\omega) = \frac{\Phi_0}{2\pi} \frac{1}{\bar{A}^*(\omega)} \sqrt{\frac{\omega}{4\pi\hbar Z_1}} \int_{-\infty}^\infty e^{i\omega t} \phi_0(t). \quad (\text{B.18})$$

We calculate now $[a_0(\omega), a_1(\omega')] + [a_1(\omega), a_0(\omega')]$, the other cases in leading order (between two creation operators, or between mixed operators) can be proved similarly. We obtain

$$\begin{aligned} [a_0(\omega), a_1(\omega')] &= \frac{\Phi_0}{\hbar\pi^2} \sqrt{\frac{\omega}{\omega'}} \frac{\bar{A}(\omega')}{\bar{A}^*(\omega)} \int_{-\infty}^\infty dt dt' \\ &\times \int_0^\infty d\omega'' \frac{\sin[\omega''(t - t')]}{\omega''} \cos[\phi_0(t') - \omega_J t'] \frac{\text{Re}[Z_t(\omega'')]}{R_Q}. \end{aligned} \quad (\text{B.19})$$

Here we have used that $[\phi_0(t), \sin \phi_0(t')] = -C(t-t')\cos \phi_0(t')$, see (B.14) and the derivation below this. We perform integration over time t , use $\text{Re}[Z_t(\omega)] = Z_1|\bar{A}(\omega)|^2$, and obtain

$$[a_0(\omega), a_1(\omega')] = i\frac{\Phi_0}{\hbar\pi}\sqrt{\frac{1}{\omega'\omega'}}\frac{Z_1\bar{A}(\omega')\bar{A}(\omega)}{R_Q}\int_{-\infty}^{\infty} dt' e^{i(\omega+\omega')t'} \cos[\phi_0(t') - \omega_J t'].$$

We observe that the result is invariant under the change $\omega \leftrightarrow \omega'$. It follows that $[a_0(\omega), a_1(\omega')] + [a_1(\omega), a_0(\omega')] = 0$, which is the desired property.

In second order the calculation goes through similar steps. We calculate first the double commutator

$$[\phi, [\sin \phi'', \cos \phi']] = C(t-t'')[\cos \phi'', \cos \phi'] + C(t-t')[\sin \phi', \sin \phi'']. \quad (\text{B.20})$$

Here we use the notation $\phi = \phi_0(t)$, $\phi' = \phi_0(t') - \omega_J t'$ and $\phi'' = \phi_0(t'') - \omega_J t''$. Using solution (17), we obtain

$$[a_0(\omega), a_2(\omega'')] = \frac{Z_1 I_c^2}{2\pi\hbar} \bar{A}(\omega)\bar{A}(\omega'')\sqrt{\frac{1}{\omega\omega''}}\int_{-\infty}^{\infty} dt' dt'' e^{i\omega' t''} \times \left[1 + \frac{\text{Sgn}(t' - t'')}{e^{\omega_c|t' - t''|} - 1}\right] \left[e^{i\omega t'} [\cos \phi'', \cos \phi'] + e^{i\omega t'} [\sin \phi', \sin \phi'']\right]. \quad (\text{B.21})$$

We observe that the total part $\propto e^{i\omega t''}$ is symmetric under the exchange $\omega \leftrightarrow \omega''$. Therefore it is canceled by the corresponding term coming from $[a_2(\omega), a_0(\omega'')]$.

The part proportional to $e^{i\omega t'}$ is equivalent to $-(1/2) \times [a_1(\omega), a_1(\omega'')]$, up to the extra part $\propto \text{Sgn}(t' - t'')$. The contribution coming from $[a_2(\omega), a_0(\omega'')]$ is obtained by changing the overall sign and performing integration over $e^{i\omega t''} e^{i\omega' t'}$, instead of $e^{i\omega' t''} e^{i\omega t'}$. We observe symmetry with respect to $t' \leftrightarrow t''$ and $[\sin \phi', \sin \phi''] \leftrightarrow [\sin \phi'', \sin \phi']$: for terms $\propto \text{Sgn}(t' - t'')$ this expression is the opposite to the original terms from $[a_0(\omega), a_2(\omega'')]$. For terms not $\propto \text{Sgn}(t' - t'')$, we have double summations of the expression form $[a_0(\omega), a_2(\omega'')]$. Thus, $[a_0(\omega), a_2(\omega'')] + [a_2(\omega), a_0(\omega'')] + [a_1(\omega), a_1(\omega'')] = 0$, which is the desired property.

Appendix C. Calculating averages $\langle e^{i\phi(t)} e^{-i\phi(t')} \rangle$

C.1. Derivation of the term $f_1(\omega)$

Using the leading order solutions for both operators $a_{\text{out}}^{(\dagger)}$ in the expression $\langle a_{\text{out}}^\dagger(\omega) a_{\text{out}}(\omega') \rangle$, we obtain a contribution for the photon flux

$$\langle a_1^\dagger(\omega) a_1(\omega') \rangle = \frac{I_c^2 Z_1}{4\hbar\pi\sqrt{\omega\omega'}} \bar{A}(\omega') \bar{A}^*(\omega) \int_{-\infty}^{\infty} dt \int_{-\infty}^{\infty} dt' e^{-i\omega t} e^{i\omega' t'} \times \langle e^{-i\omega_J(t-t')} e^{i\phi_0(t)} e^{-i\phi_0(t')} + e^{i\omega_J(t-t')} e^{-i\phi_0(t)} e^{i\phi_0(t')} \rangle. \quad (\text{C.1})$$

Here we have used the fact that expectation values of the form $\langle e^{i\phi_0(t)} e^{i\phi_0(t')} \rangle$ are zero due to random phase fluctuations. Also contributions such as $\langle a_0(\omega) a_1(\omega') \rangle$ vanish for the same reason. We use now the following property of bosonic operators [2],

$$\langle e^{i\phi_0(t)} e^{-i\phi_0(t')} \rangle = \langle e^{-i\phi_0(t)} e^{i\phi_0(t')} \rangle = e^{J(t-t')}, \quad (\text{C.2})$$

where $J(t) = \langle [\phi_0(t) - \phi_0(0)]\phi_0(0) \rangle$. We then perform a change of variables, $x = t - t'$, $y = (t + t')/2$, do integrations over x and y , and obtain

$$\langle a_1^\dagger(\omega)a_1(\omega') \rangle = \delta(\omega - \omega') \frac{\pi I_c^2 Z_1 |\bar{A}(\omega)|^2}{\omega} [P(\hbar\omega_J - \hbar\omega) + P(-\hbar\omega_J - \hbar\omega)]. \quad (\text{C.3})$$

C.2. Derivation of the term $f_{\text{in}}(\omega)$

We derive now the inelastic reflection of thermal photons, $f_{\text{in}}(\omega)$. To do this we take use of the zeroth-order solution (B.18) and the second-order solution (17). We obtain

$$\begin{aligned} \langle a_2^\dagger(\omega)a_0(\omega'') \rangle &= \frac{R_Q I_c^2 \bar{A}^*(\omega)}{8\pi^2 \bar{A}^*(\omega'')} \sqrt{\frac{\omega''}{\omega}} \int_{-\infty}^{\infty} dt dt' dt'' \left[1 + \frac{\text{Sgn}(t - t')}{e^{\omega_c|t-t'|} - 1} \right] \\ &\times \langle \{ \cos[\phi_0(t') - \omega_J t'] \sin[\phi_0(t) - \omega_J t] - \text{h.c.} \} \phi_0(t'') \rangle. \end{aligned} \quad (\text{C.4})$$

The next step is to calculate the ensemble average. By applying Wick's theorem we obtain

$$\langle e^{\pm i\phi_0(t)} e^{\mp i\phi_0(t')} \phi_0(t'') \rangle = \pm i [J(t - t'') - J(t' - t'')] e^{J(t-t')}.$$

We also have $\langle e^{\pm i\phi_0(t)} e^{\pm i\phi_0(t')} \rangle = 0$. These relations lead to

$$\begin{aligned} \langle \{ \cos[\phi(t') - \omega_J t'] \sin[\phi(t) - \omega_J t] - \text{h.c.} \} \phi(t'') \rangle \\ = \frac{1}{2} \cos[\omega_J(t - t')] [J(t - t'') - J(t' - t'')] \left(e^{J(-t+t')} - e^{J(t-t')} \right). \end{aligned} \quad (\text{C.5})$$

We can perform integration over t'' by using

$$J(t) = 2 \int_0^{\infty} \frac{d\omega}{\omega} \frac{\text{Re}[Z_t(\omega)]}{R_Q} \left\{ \coth\left(\frac{1}{2}\beta\hbar\omega\right) [\cos(\omega t) - 1] - i \sin(\omega t) \right\}$$

and obtain

$$\begin{aligned} \int_{-\infty}^{\infty} e^{i\omega'' t''} [J(t - t'') - J(t' - t'')] \\ = 2\pi \frac{\text{Re}[Z_t(\omega'')]}{R_Q \omega''} \left\{ \coth\left(\frac{1}{2}\beta\hbar\omega''\right) [e^{i\omega'' t} - e^{i\omega'' t'}] - [e^{i\omega'' t} - e^{i\omega'' t'}] \right\}. \end{aligned}$$

The term inside the last parentheses can be put into the form

$$4i \left(\frac{1}{e^{\beta\hbar\omega''} - 1} \right) \sin\left(\omega'' \frac{t - t'}{2}\right) \exp\left[i\omega'' \frac{t + t'}{2}\right].$$

Using these relations, we obtain

$$\begin{aligned} \langle a_2^\dagger(\omega)a_0(\omega'') \rangle &= i \frac{I_c^2 \bar{A}^*(\omega)}{2\pi \hbar \bar{A}^*(\omega'')} \sqrt{\frac{\omega''}{\omega}} \frac{\text{Re}[Z_t(\omega'')]}{\omega''} \\ &\times \int_{-\infty}^{\infty} dt dt' e^{-i\omega t} e^{i\omega'' t''} \cos[\omega_J(t - t')] [e^{J(t'-t)} - e^{J(t-t')}] \\ &\times \sin\left(\omega'' \frac{t - t'}{2}\right) \frac{1}{e^{\beta\hbar\omega''} - 1} \left[1 + \frac{\text{Sgn}(t - t')}{e^{\omega_c|t-t'|} - 1} \right]. \end{aligned} \quad (\text{C.6})$$

For the last two time integrations we do a change of variables $x = t - t'$ and $y = (t + t')/2$. The resulting y -dependence is in a factor $\exp[iy(\omega'' - \omega)]$. The integration over y leads to the factor $2\pi\delta(\omega - \omega'')$. Performing integration over ω'' and division by 2π (to obtain f_{in}), one gets

$$\int_0^\infty d\omega'' \frac{1}{2\pi} \langle a_2^\dagger(\omega) a_0(\omega'') \rangle = \frac{2I_c^2}{\hbar} f_0(\omega) \frac{\text{Re}[Z_t(\omega)]}{\omega} \times \int_{-\infty}^\infty dx \cos(\omega_J x) \text{Im}[e^{J(x)}] e^{-i\frac{x\omega}{2}} \sin\left(\frac{\omega x}{2}\right) \left[1 + \frac{\text{Sgn}(x)}{e^{\omega_c|x|} - 1}\right]. \quad (\text{C.7})$$

Adding this with the contribution $\langle a_0^\dagger(\omega) a_2(\omega'') \rangle = \langle a_2^\dagger(\omega'') a_0(\omega) \rangle^*$, and using $\omega = \omega''$, one sees that only two times the real part of (C.7) survives. Thus,

$$f_{\text{in}}(\omega) = f_0(\omega) \frac{2I_c^2}{\hbar\omega} \text{Re}[Z_t(\omega)] \int_{-\infty}^\infty dx \text{Im}[e^{J(x)}] \cos(\omega_J x) \sin(\omega x) \left[1 + \frac{\text{Sgn}(x)}{e^{\omega_c|x|} - 1}\right]. \quad (\text{C.8})$$

We know that $J(-x) = J^*(x)$, and therefore $\text{Im}[e^{J(-x)}] = -\text{Im}[e^{J(x)}]$. Therefore the part $\propto \text{Sgn}(x)$ cancels out due to symmetry reasons. Because only $e^{J(x)}$ is a complex number, the result does not change if we take the imaginary part over the whole expression (without the part $\propto \text{Sgn}(x)$), instead of only over $e^{J(x)}$. This leads to result (29).

Appendix D. Estimating higher-order coherences up to second order in I_c

We want to calculate expressions such

$$\langle a_{\text{out}}^\dagger(\omega) a_{\text{out}}^\dagger(\omega') a_{\text{out}}(\omega'') a_{\text{out}}(\omega''') \rangle, \quad (\text{D.1})$$

up to second order in I_c . We do this by inserting the first-order solution $a_1^{(\dagger)}$ and the zeroth-order solution $a_0^{(\dagger)}$ both twice into the four operators $a_{\text{out}}^{(\dagger)}$. We neglect the contribution if using the second-order solution a_2^\dagger once, as this is proportional to $f_0(\omega)$. We will also neglect backward directed Cooper-pair tunneling, i.e. we take the approximation $a_1(\omega) \propto \int dt e^{i(\omega - \omega_1)t} e^{i\phi_0(t)}$ and neglect terms of type $\propto \int dt e^{i(\omega + \omega_1)t} e^{-i\phi_0(t)}$. Such tunneling against the voltage is well suppressed by the temperature.

We make use of the following result for the ensemble average of bosonic operators ϕ :

$$\langle e^{-i\phi} \phi' \phi'' e^{i\phi'''} \rangle = \langle e^{-i\phi} e^{i\phi'''} \rangle \{ \langle \phi' \phi'' \rangle + [\langle \phi'' \phi''' \rangle - \langle \phi \phi'' \rangle] [\langle \phi \phi' \rangle - \langle \phi' \phi''' \rangle] \}. \quad (\text{D.2})$$

Here we use the notation $\phi' = \phi_0(t')$ and similarly for others. The result can be derived by expressing the exponential functions as a power series and applying Wick's theorem. Important here is that the order of the operators ϕ^i stays the same when contracted into the pairs. This is then also valid for permutations of the initial operators. The result (D.2) is also immune to exchanging the signs in the exponents.

D.1. Intensity cross-correlations

We consider first the correlator

$$\langle a_{\text{out}}^\dagger(\omega) a_{\text{out}}(\omega') a_{\text{out}}^\dagger(\omega'') a_{\text{out}}(\omega''') \rangle. \quad (\text{D.3})$$

Once we obtain an expression for this, the other orderings of the operators $a_{\text{out}}^{(\dagger)}$ can be deduced by using general relations for the field operators, equation (8). We need to calculate the sum of all the orderings

$$\langle e^{-i\phi} \phi' \phi'' e^{i\phi'''} \rangle + \langle e^{-i\phi} e^{i\phi'''} \phi'' \phi' \rangle + \langle \phi'' \phi' e^{-i\phi} e^{i\phi'''} \rangle + \langle \phi'' e^{i\phi'''} e^{-i\phi} \phi' \rangle.$$

However, it turns out that only the first of these four terms is important, as the other terms are proportional to $f_0(\omega)$ and can be neglected. This can be understood by rewriting the ensemble average with the help of a formal density matrix $\hat{\rho}$ of the unperturbed system, $\text{Tr} \{ a(\omega') a^\dagger(\omega'') a(\omega''') \hat{\rho} a^\dagger(\omega) \}$: tunneling with radiation ($\propto e^{\pm i\phi_0(t)}$) has to be inserted around the density matrix, otherwise the result is zero at $T = 0$.

To calculate (D.3), the difficulty is to perform integration over all times of the term

$$\langle e^{-i\phi} \phi' \phi'' e^{i\phi'''} \rangle e^{i(-\omega+\omega_1)t+i\omega't'-i\omega''t''+i(\omega''-\omega_1)t''}. \quad (\text{D.4})$$

In result (D.2) the first term inside the brackets is the easiest to calculate, as the time-dependent terms are only functions of $t - t'''$ or $t' - t''$. Twice we do similar change of variables as when calculating $f_t(\omega)$ (appendix C) and obtain the first contribution for the term (D.4),

$$(2\pi)^2 \int_{-\infty}^{\infty} dx_1 \int_{-\infty}^{\infty} dx_2 e^{J(x_1)} p(x_2) e^{ix_1(\omega_1-\omega)} e^{ix_2\omega'} \delta(\omega-\omega''') \delta(\omega'-\omega'') = (2\pi)^2 [2\pi \hbar P(\hbar\omega_1 - \hbar\omega)] \\ \times \left[4\pi \frac{1}{\omega'} \frac{\text{Re}[Z_t(\omega')]}{R_Q} \right] \delta(\omega-\omega''') \delta(\omega'-\omega''). \quad (\text{D.5})$$

Here we mark $p(t' - t'') \equiv \langle \phi(t') \phi(t'') \rangle$ and it is determined by equation (15). We have neglected a contribution proportional to $f_0(\omega)$.

Only the last term, proportional to $\langle \phi \phi'' \rangle \langle \phi' \phi''' \rangle$, gives another finite contribution at $T = 0$,

$$2\pi [2\pi \hbar P(\hbar\omega_1 - \hbar\omega - \hbar\omega'')] \left[4\pi \frac{1}{\omega'} \frac{\text{Re}[Z_t(\omega')]}{R_Q} \right] \left[4\pi \frac{1}{\omega''} \frac{\text{Re}[Z_t(\omega'')]}{R_Q} \right] \delta(-\omega + \omega' - \omega'' + \omega'''). \quad (\text{D.6})$$

We note that in this case the operators of the same type are paired [$a(\omega') \leftrightarrow a(\omega''')$, $a^\dagger(\omega) \leftrightarrow a^\dagger(\omega'')$]. To obtain the expression for (D.3) we sum up these two results and multiply them with $\tilde{A} \sqrt{\frac{\omega' \omega''}{\omega \omega'''}} \left(\frac{I_c}{8e\pi} \right)^2$, where

$$\tilde{A} = \frac{\bar{A}^*(\omega) \bar{A}(\omega''')}{\bar{A}^*(\omega') \bar{A}(\omega'')}. \quad (\text{D.7})$$

We obtain the intensity cross-correlations up to second order in I_c ,

$$2\pi \frac{I_c^2}{2\omega} P(\hbar\omega_1 - \hbar\omega) \text{Re}[Z_t(\omega)] \delta(\omega-\omega''') \delta(\omega'-\omega'') + \tilde{A} \delta(\omega-\omega'+\omega''-\omega''') \frac{2\pi I_c^2}{\sqrt{\omega \omega' \omega'' \omega'''}} \\ \times P[\hbar(\omega_1 - \omega - \omega'')] \left\{ \frac{\text{Re}[Z_t(\omega')] \text{Re}[Z_t(\omega'')]}{R_Q} \right\}. \quad (\text{D.8})$$

D.2. Second-order coherence $G^{(2)}$

We consider now the expectation value $\langle a^\dagger(\omega)a^\dagger(\omega')a(\omega'')a(\omega''') \rangle$. By using the identity $[a_{\text{out}}(\omega), a_{\text{out}}^\dagger(\omega')] = \delta(\omega - \omega')$ and doing the exchange $\omega' \leftrightarrow \omega''$ in term (D.8), we obtain the result

$$\langle a^\dagger(\omega)a^\dagger(\omega')a(\omega'')a(\omega''') \rangle = \tilde{A}(\omega, \omega'', \omega', \omega''')\delta(\omega + \omega' - \omega'' - \omega''')\frac{2\pi I_c^2}{\sqrt{\omega\omega'\omega''\omega'''}} \times P[\hbar(\omega_J - \omega - \omega')] \left\{ \frac{\text{Re}[Z_t(\omega')]\text{Re}[Z_t(\omega'')]}{R_Q} \right\}. \quad (\text{D.9})$$

This can also be derived through a direct calculation, as was done for the intensity cross-correlator.

D.3. Cauchy–Schwarz inequality

The Cauchy–Schwarz inequality compares intensity correlations with the second-order coherence. We calculate these in a small frequency interval $\Delta\omega$ around the frequencies ω_a and ω_b . This assumes a filtering of the measured output signal into these frequencies (intensity-correlations).

We integrate result (D.9) over four frequencies, each of them having the interval $\omega \in [\omega_a - \Delta\omega/2, \omega_a + \Delta\omega/2]$. We obtain by assuming a small $\Delta\omega$,

$$G^{(2)}(0) \approx \frac{2\pi I_c^2 \Delta\omega^3}{\omega_a^2 R_Q} P[\hbar(\omega_J - 2\omega_a)] [\text{Re}[Z_t(\omega_a)]]^2. \quad (\text{D.10})$$

Here we have used $\tilde{A}(\omega_a, \omega_a, \omega_a, \omega_a) = 1$. Similarly for the contribution at ω_b .

The cross-correlations between the two frequencies, $\omega_a - \omega_b \gg \Delta\omega$, give

$$\int_{\omega_a - \Delta\omega/2}^{\omega_a + \Delta\omega/2} d\omega d\omega' \int_{\omega_b - \Delta\omega/2}^{\omega_b + \Delta\omega/2} d\omega'' d\omega''' \langle a^\dagger(\omega)a(\omega')a^\dagger(\omega'')a(\omega''') \rangle \approx \tilde{A}(\omega_a, \omega_a, \omega_b, \omega_b) \frac{2\pi I_c^2 \Delta\omega^3}{\omega_a \omega_b R_Q} P[\hbar(\omega_J - \omega_a - \omega_b)] \text{Re}[Z_t(\omega_a)] \text{Re}[Z_t(\omega_b)]. \quad (\text{D.11})$$

We notice from (D.7) that also $\tilde{A}(\omega_a, \omega_a, \omega_b, \omega_b) = 1$. (Actually an additional factor 2/3 appears for both cross- and autocorrelations, due to the specific form of the bandwidth cutoff, but is neglected here for simplicity.)

D.4. Bunching for $Z_0 = Z_1$

For the free-space configuration ($Z_0 = Z_1$) we have a simple result $\tilde{A} = \mathcal{C}^*(\omega')\mathcal{C}(\omega'')/\mathcal{C}^*(\omega)\mathcal{C}(\omega''')$. In the following we will assume that $\omega_J \ll \omega_c$, so that $\tilde{A} = 1$

and $\text{Re}[Z(\omega)] = Z_0$. One obtains for the second-order coherence (when integrated over all frequencies)

$$\begin{aligned} G^{(2)}(0) &= \frac{2\pi}{R_Q} \left(\frac{I_c \hbar Z_0^2}{4\pi} \right)^2 \int_0^\infty d\omega \int_0^\infty d\omega' \int_0^{\omega+\omega'} d\omega'' P[\hbar(\omega_J - \omega - \omega')] \\ &= \frac{2\pi}{R_Q} \left(\frac{I_c \hbar Z_0^2}{4\pi} \right)^2 \int_0^\infty d\omega \int_0^\infty d\omega' (\omega + \omega') P[\hbar(\omega_J - \omega - \omega')]. \end{aligned} \quad (\text{D.12})$$

We now do a change of variables: $s = \omega + \omega'$, $t = (\omega - \omega')/2$, and get

$$\begin{aligned} G^{(2)}(0) &= \frac{2\pi}{R_Q} \left(\frac{I_c \hbar Z_0^2}{4\pi} \right)^2 \int_0^\infty ds \int_{-s/2}^{s/2} dt s P[\hbar(\omega_J - s)] \\ &= \frac{2\pi}{R_Q} \left(\frac{I_c \hbar Z_0^2}{4\pi} \right)^2 \int_0^\infty ds s^2 P[\hbar(\omega_J - s)]. \end{aligned} \quad (\text{D.13})$$

On the other hand, in the same approximation the first-order coherence is

$$g_t^{(1)}(0) = \frac{I_c^2 Z_0^2}{4} \frac{e^{-2\gamma\rho}}{\Gamma(1+2\rho)} \left(\frac{\pi\rho\hbar\omega_J}{4E_C} \right)^{2\rho}. \quad (\text{D.14})$$

This gives

$$g_t^{(2)}(0) = \left(\frac{\hbar\omega_J}{\pi E_J} \right)^2 \left[\pi\rho \frac{\hbar\omega_J}{4E_C} \right]^{-2\rho} \frac{\Gamma(1+2\rho)e^{2\gamma\rho}}{1+3\rho+2\rho^2}. \quad (\text{D.15})$$

For small ρ we obtain $g_t^{(2)}(0) = (\hbar\omega_J/\pi E_J)^2$. For a general time τ we substitute

$$s^2 \rightarrow \left(\frac{2}{\tau} \right)^2 \sin^2 \left(\frac{\tau s}{2} \right), \quad (\text{D.16})$$

in equation (D.13).

Let us consider a restricted region of frequency interval, $\omega_0 - \Delta\omega/2 < \omega < \omega_0 + \Delta\omega/2$, for all frequencies. We obtain a new integration range

$$\int_{2\omega_0}^{2\omega_0+\Delta\omega} ds \int_{s/2-\omega_0-\Delta\omega/2}^{-(s/2-\omega_0)+\Delta\omega/2} dt \int_{s-\omega_0-\Delta\omega/2}^{\omega_0+\Delta\omega/2} d\omega'' + \int_{2\omega_0-\Delta\omega}^{2\omega_0} ds \int_{-(s/2-\omega_0)-\Delta\omega/2}^{s/2-\omega_0+\Delta\omega/2} dt \int_{\omega_0-\Delta\omega/2}^{s-\omega_0+\Delta\omega/2} d\omega''.$$

Since the integrant (D.12) is independent of both ω'' and t , the integration range gets the form

$$\int_{2\omega_0-\Delta\omega}^{2\omega_0+\Delta\omega} ds (-|2\omega_0 - s| + \Delta\omega)^2,$$

and one obtains for the corresponding second-order coherence

$$G_t^{(2)}(0) = \frac{2\pi}{R_Q} \left(\frac{I_c \hbar Z_0^2}{4\pi} \right)^2 \int_{2\omega_0-\Delta\omega}^{2\omega_0+\Delta\omega} ds (-|2\omega_0 - s| + \Delta\omega)^2 P[\hbar(\omega_J - s)].$$

For low temperatures we have $P(E) \approx 0$ for $E < -k_B T$. Therefore the result is practically zero if the lower limit of integration is above ω_J . An optimal result is obtained for the integration

range that covers symmetrically the $P(E)$ peak at $E = 0$, i.e. for $\omega_0 = \omega_J/2$. For small $\Delta\omega$, but still larger than the thermal width Γ , the $P(E)$ -function can be approximated as $\delta(E)$, and the integration gives in this case ($\rho \ll 1$, $\Delta\omega \gg \Gamma$)

$$G_t^{(2)}(0) = \frac{2\pi\hbar}{R_Q} \left(\frac{I_c Z_0^2}{4\pi} \right)^2 \Delta\omega^2 = \left(\frac{I_c^2 Z_0^2}{4} \right)^2 \left(\frac{\hbar\Delta\omega}{\pi E_J} \right)^2.$$

This leads to result (44).

References

- [1] Devoret M H, Esteve D, Grabert H, Ingold G-L, Pothier H and Urbina C 1990 *Phys. Rev. Lett.* **64** 1824
- [2] Ingold G-L and Nazarov Y V 1992 *Single Charge Tunneling: Coulomb Blockade Phenomena in Nanostructures* ed H Grabert and M H Devoret (New York: Plenum) pp 21–107
- [3] Holst Esteve, Urbina C and Devoret M H 1994 *Phys. Rev. Lett.* **73** 3455
- [4] Leppäkangas J, Thuneberg E, Lindell R and Hakonen P 2006 *Phys. Rev. B* **74** 054504
- [5] Bretheau L, Girit Ç Ö, Pothier H, Esteve D and Urbina C 2013 *Nature* **499** 312
- [6] Hofheinz M, Portier F, Baudouin Q, Joyez P, Vion D, Bertet P, Roche P and Esteve D 2011 *Phys. Rev. Lett.* **106** 217005
- [7] Leppäkangas J, Johansson G, Marthaler M and Fogelström M 2013 *Phys. Rev. Lett.* **110** 267004
- [8] Padurariu C, Hassler F and Nazarov Y V 2012 *Phys. Rev. B* **86** 054514
- [9] Gramich V, Kubala B, Rocher S and Ankerhold J 2013 *Phys. Rev. Lett.* **111** 247002
- [10] Armour A D, Blencowe M P, Bahimi E and Rimberg A J 2013 *Phys. Rev. Lett.* **111** 247001
- [11] Johansson J R, Johansson G, Wilson C M and Nori F 2010 *Phys. Rev. A* **82** 052509
- [12] Wallquist M, Shumeiko V S and Wendin G 2006 *Phys. Rev. B* **74** 224506
- [13] Peskin M E and Schroeder D V 1995 *An Introduction to Quantum Field Theory* (Boulder, CO: Westview)
- [14] Likharev K K 1986 *Dynamics of Josephson Junctions and Circuits* (New York: Gordon and Breach)
- [15] Loudon R 2010 *The Quantum Theory of Light* (New York: Oxford University)
- [16] Grabert H, Schramm P and Ingold G-L 1988 *Phys. Rep.* **168** 115
- [17] Grabert H, Ingold G-L and Paul B 1998 *Europhys. Lett.* **44** 360
- [18] Dahm A J, Denenstein A, Langenberg D N, Parker W H, Rogovin D and Scalapino D J 1969 *Phys. Rev. Lett.* **22** 1416
- [19] Stephen M J 1968 *Phys. Rev. Lett.* **21** 1629
- [20] Lee P A and Scully M O 1971 *Phys. Rev. B* **3** 769
- [21] Rogovin D and Scalapino D J 1974 *Ann. Phys.* **86** 1
- [22] Levinson Y 2003 *Phys. Rev. B* **67** 184504
- [23] Koch R H, Van Harlingen D J and Clarke J 1980 *Phys. Rev. Lett.* **45** 2132
- [24] Grabert H and Ingold G-L 2002 *Europhys. Lett.* **58** 429
- [25] Ingold G-L and Grabert H 1999 *Phys. Rev. Lett.* **83** 3721
- [26] Scully M O and Zubairy M S 1997 *Quantum Optics* (Cambridge: Cambridge University Press)
- [27] da Silva M P, Bozyigit D, Wallraff A and Blais A 2010 *Phys. Rev. A* **82** 043804
- [28] Walls D F and Milburn G J 2008 *Quantum Optics* (Berlin: Springer)
- [29] Miranowicz A, Bartkowiak M, Wang X, Liu Y and Nori F 2010 *Phys. Rev. A* **82** 013824